28th Numerical Towing Tank Symposium (NuTTS)
19-21 October 2026 - Mülheim an der Ruhr, Germany

Numerical and Experimental Investigation of Inland Waterway Ship–Bank Interaction Using Scale-Resolving Simulation

Melissa Böhm[1,2], **Lahbib Zentari**[1], **Bettar Ould el Moctar**[2], and **Benjamin Friedhoff**[3]
[1]Bundesanstalt für Wasserbau (BAW), Karlsruhe/Germany,
[2]Department of Autonomous and Energy-Efficient Maritime Technologies, Technical University of Berlin, Berlin/Germany,
[3]Development Center for Ship Technology and Transport Systems, Duisburg/Germany
melissa.boehm@baw.de

1 Introduction

Climate change is expected to intensify low-water events, leading to increasingly restricted navigational conditions on inland waterways. This trend increases the difficulty of ship navigation, rendering it more challenging. To assess safety and ease of manoeuvring under these circumstances, accurate navigability analyses are necessary. These rely on mathematical manoeuvring models that take into account ship–waterway interactions, see Eloot and Vantorre (2011). Given the challenges posed by inland waterway vessels and the extreme confinement they are subjected to, Computational Fluid Dynamic (CFD) offers a powerful means of investigating in depth the complex hydrodynamic phenomena governing such ships when travelling near a bank with low under keel clearance. To this end, we analysed a representative case with lateral confinement in very shallow water, both experimentally and numerically. The focus is on comparing two numerical approaches using the following turbulence models: Unsteady Reynolds-Averaged Navier-Stokes (URANS) with the two-equation $k-\omega-$SST as formulated by Menter (1994), and the scale-resolving hybrid Improved Delayed Detached Eddy Simulation (IDDES) model by Gritskevich et al. (2012). We compared their computational costs and evaluated how well the simulated results agreed with the experimental data in terms of hydrodynamic forces and moments, as well as pressure distribution on the hull. The IDDES computations showed the best agreement with the experimental data, albeit at a higher computational cost.

2 Test case and Setup

The investigated test case was the inland waterway ship benchmark introduced by Mucha et al. (2017), at a scale of $\lambda = 16$. It represents a typical 135 m long cargo vessel routinely navigating the Rhine river. Main particulars are detailed in Table 1.

The experimental campaign for investigating bank effects was carried out at the Development Centre for Ship Technology and Transport Systems (DST) in Duisburg, Germany. The test basin has a length of 200 m and a breadth of 9.80 m. For this campaign, a vertical wall 55.35 m long was installed longitudinally to also capture unsteady effects in ship–bank interactions, forming a channel with a width of 6.385 m. The model ship was towed at a constant velocity U_0 of $0.556\,\mathrm{m\,s^{-1}}$ and gradually decelerated after passing the bank.

Figure 2 schematises the experimental setup. The ship, shown in yellow, started 65.00 m behind the wall and was gradually accelerated until reaching the constant speed U_0; it was then decelerated once its stern passed the far extremity of the bank, at 120.35 m from the starting position. The ship travelled with its starboard side close to the wall. Transducers mounted on the ship measured the hydrodynamic longitudinal force X, lateral force Y, and yaw moment N, as well as propeller and duct thrust, T_P and T_D respectively.

The experimental campaign covered various water depth-to-draft ratios h/T, wall distance-to-ship-length ratios d/L_{PP}, and ship speeds U_0, where d is the distance from the wall to midships, L_{PP} the ship length, h the water depth, and T the ship draft. In the present paper, we focused on the worst-case scenario, namely $h/T = 1.2$ and $d/L_{PP} = 0.1$, representing the highest confinement in the test matrix. To assess repeatability, selected tests were run at least twice.

A detailed description of the experimental setup, along with an in-depth uncertainty analysis, will be the subject of a future publication. Figure 2 shows a photograph of the experimental campaign during a test run.

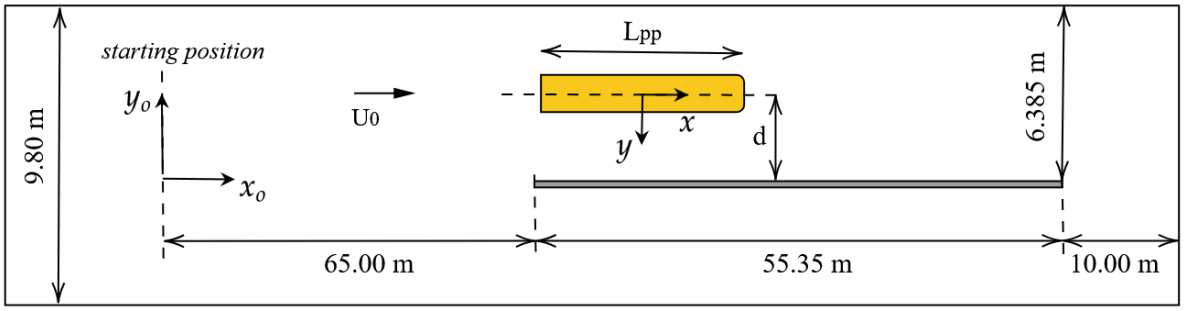


Fig. 1: Setup of the model experiments in the shallow water basin of the DST

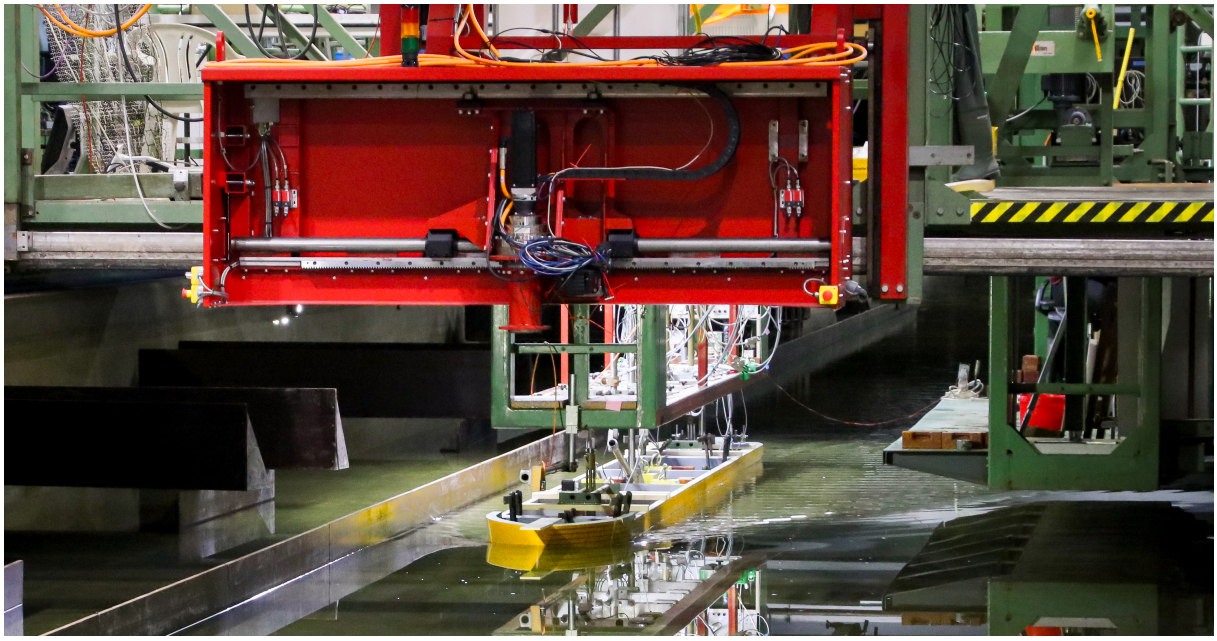


Fig. 2: Model ship and towing carriage during the model experiments in the shallow water basin of the DST

3 Numerical procedure

We performed our numerical flow simulations using the commercial solver Simcenter STAR-CCM+ Siemens (2023). The main objective of the present study was to assess different turbulence modelling approaches regarding accuracy and computational efficiency. For this purpose, we employed the k-ω SST turbulence model for closure, and the hybrid RANS/LES IDDES model. All simulations were conducted as unsteady simulations using the double-body method, motivated by the relatively low Froude number $F_r < 0.1$ and the correspondingly small free-surface disturbance. The trim and sinkage in the simulation are based on averaged model test values.

Figure 3 illustrates the computational domain and the boundary conditions. The domain inflow was specified as a velocity inlet, and the outflow as a pressure outlet. The top boundary was specified as a symmetry plane, and the sides and bottom as no-slip walls, with the relative velocity at the bottom and sides set to the ship speed. The ship hull was also specified as a

Table 1: Main dimensions of the testcase and its appendages under design loading conditions, in both full-scale and model-scale, based on Mucha (2017).

Description	**Symbol**	**Unit**	**Full scale**	**Model scale**
Scale factor	λ	–	1	16
Length of waterline	L_{WL}	m	134.42	8.4013
Length between perpendiculars	L_{PP}	m	135.00	8.4375
Breadth	B	m	11.44	0.7150
Draft	T	m	3.5	0.2188
Wetted surface	S_W	m^2	2376.1	9.2817
Volumetric displacement	∇	m^3	4992	1.2187
Block coefficient	C_B	–	0.92	0.92
Number of propeller blades	Z	–	4	4
Propeller diameter	D_P	m	1.6	0.1

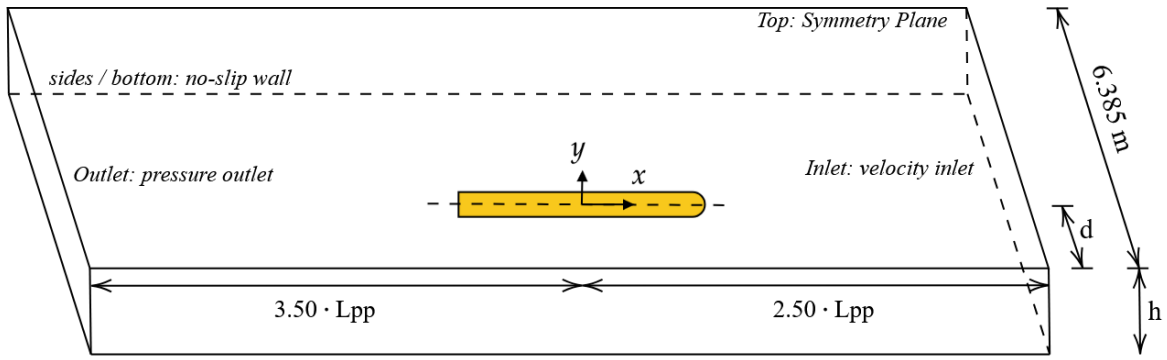


Fig. 3: Computational domain, that represents the period during which the ship travels alongside the wall in the 6.385-metre-wide canal during the experiments.

no-slip wall, with zero tangential velocity. The propeller was modelled using the reference frame method.

For all simulations, a time step of $\Delta t = 0.005\,\mathrm{s}$ and a base grid size of $\Delta x = 0.064\,\mathrm{m}$ were chosen, with second-order temporal discretization applied throughout. The hexahedral trimmed cell mesher was adopted to build an unstructured mesh. Areas of high pressure and velocity gradients were expected around the bow and stern of the model, near the propulsion and steering devices, and between the model and the bank. Accordingly, the grid was refined in these regions. The complete mesh comprised approximately 12.7 million cells, of which 2.3 million were located within the propeller subdomains. The boundary layer on the tank bottom and hull was fully resolved, with y^+ values below unity.

4 Results and Discussion

The main results of our investigations are presented in Figure 4. This figure shows a comparison between the numerical and experimental results for the integral lateral force Y, and yaw moment N acting on the ship as a system, i.e., including steering and propulsive forces. In this figure, the grey line represents the experimental time series, the orange line the results computed using the RANS model; the green line those obtained using the IDDES model. The results shown in this figure compare the time history of forces as the ship passed along the bank. Although the experimental time series was comparatively noisy, the agreement between numerical and experimental results was satisfactory for both models. Table 2 shows a quantitative comparison

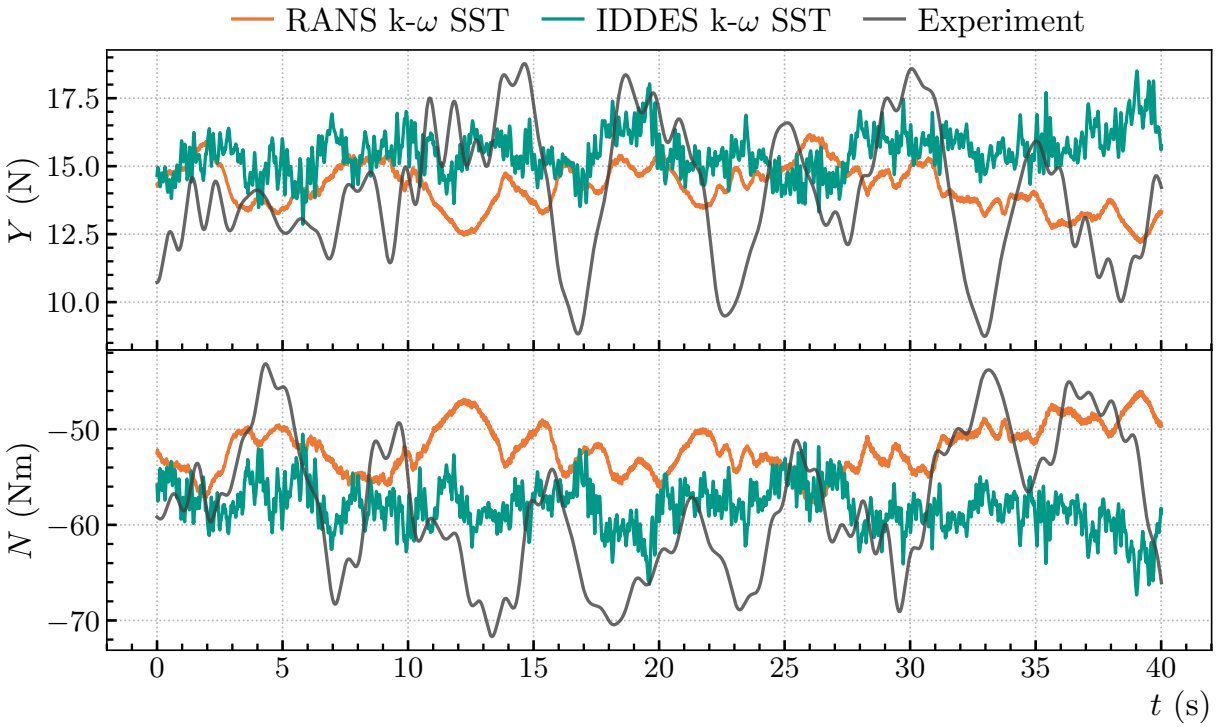


Fig. 4: Time series of hydrodynamic forces Y and N at $d/L_{PP} = 0.1$, $h/T = 1.2$ and $U_0 = 0.556\ \mathrm{m\,s^{-1}}$ comparing two numerical approaches with the experiment.

Table 2: Mean experimental and numerical results for Y and N, based on one experimental test run and two numerical approaches, with percentage differences relative to the experimental results (baseline).

	Y **(N)**	N **(Nm)**	ΔY **(%)**	ΔN **(%)**
Experiment	13.642	-56.085	–	–
RANS k-ω SST	14.268	-52.251	4.59	-6.84
IDDES k-ω SST	15.305	-57.592	12.19	2.69

between the mean force values, with the experimental results serving as the baseline. The best agreement was achieved using the IDDES method for the yaw moment N, while the RANS methodologies offered the best agreement for Y. However, the experimental methodology, which involved a sudden variation in the wall, may have introduced inherent unsteady effects that were not accounted for in the simulations. Indeed, our simulations only considered the quasi-steady case, i.e., a ship sailing straight at a fixed distance from the wall.

The differences between the computed forces obtained using each turbulence model may be explained by comparing the pressure distribution on the hull. Figure 5 and 6 shows the pressure coefficient distribution on the bow and stern region for both considered simulations. In the bow area, there was no clear difference between the approaches: the bank effect was equally visible in both, characterized by the shifted low-pressure zone on the starboard side, resulting from the pressure difference induced by the bank. In the aft region, however, where the flow was rather complex due to the rotating propeller and the complex ship–bank interactions, the pressure distribution revealed a clear difference between the methodologies. Given the scale-resolving nature of the IDDES simulation, its results showed a markedly different pressure field. Nonetheless, these instantaneous snapshots offer only a qualitative comparison.

For the same number of computational nodes on our high-performance computer the RANS

$k-\omega-$SST and IDDES simulations required approximately 3.2 and 3.5 hours of computational time, respectively, for a simulated time of 100 s.

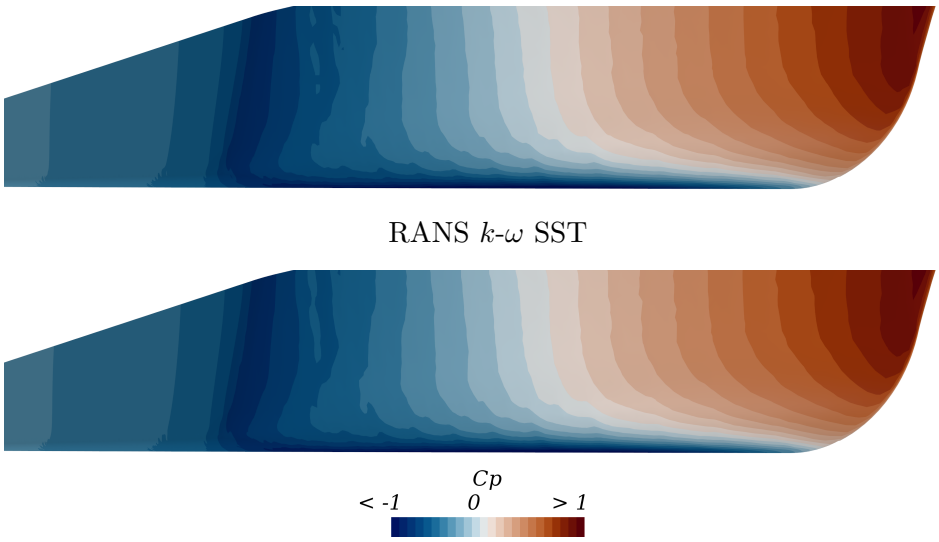


Fig. 5: Distribution of pressure coefficient on ship hull at $d/L_{PP} = 0.1$, $h/T = 1.2$ and $U_0 = 0.556\ \mathrm{m\,s^{-1}}$ for both numerical approaches.

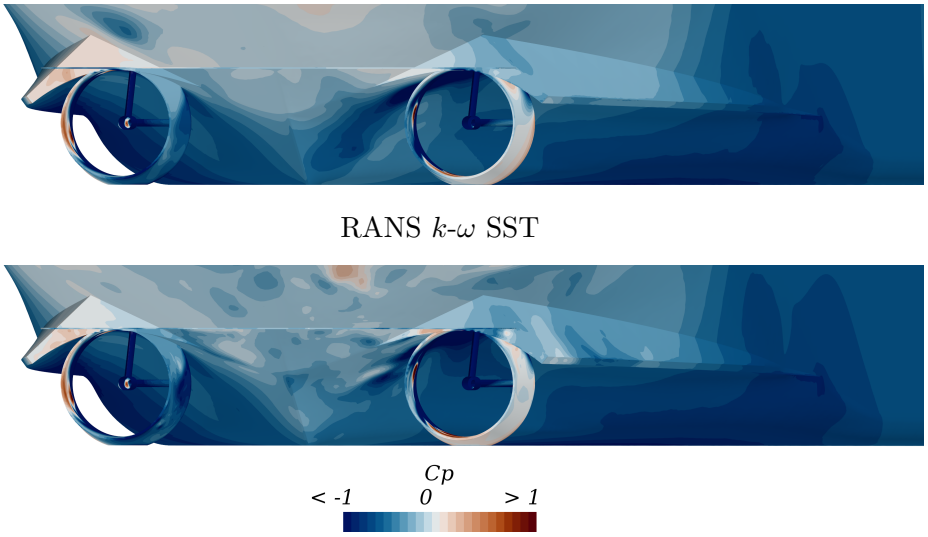


Fig. 6: Distribution of pressure coefficient on ship hull at $d/L_{PP} = 0.1$, $h/T = 1.2$ and $U_0 = 0.556\ \mathrm{m\,s^{-1}}$ for both numerical approaches.

5 Conclusion and Future Work

In this study, we investigated the influence of turbulence modelling on the prediction of ship–bank interaction effects for a representative inland waterway ship case, comparing a RANS approach and the hybrid IDDES method against experimental data. For this particular case, IDDES offered the most promising results for the prediction of the yaw moment N, which is of primary importance for navigability assessments. The RANS methodology, on the other hand, provided the best agreement for the lateral force Y. Nevertheless, the large variances observed in the

experimental time series indicate that a definitive assessment of whether RANS underpredicts the forces would require the study to span multiple bank distances and water depths. Future work will therefore focus on extending the present analysis to other bank distances and water depths, in order to assess the robustness of these findings across the confinement conditions relevant to inland waterway navigation. Additionally, the modelling of the complete unsteady manoeuvre, including the ship's approach to and departure from the bank, will be considered to capture the unsteady effects inherent to the experimental methodology, which were not accounted for in the present quasi-steady simulations.

Acknowledgements

This study originated from a joint research project between the Federal Waterways Engineering and Research Institute (Bundesanstalt für Wasserbau, BAW), the Department of Autonomous and Energy-Efficient Maritime Technologies of the University of Berlin and the Development Center for Ship Technology and Transport Systems (DST).

References

Eloot, K., Vantorre, M., 2011. Ship behaviour in shallow and confined water: an overview of hydrodynamic effects through efd, in: Assessment of stability and control prediction methods for NATO air and sea vehicles, NATO. Research and Technology Organisation (RTO). pp. 1–20.

Gritskevich, M.S., Garbaruk, A.V., Schütze, J., Menter, F.R., 2012. Development of ddes and iddes formulations for the k-ω shear stress transport model. Flow, Turbulence and Combustion 88, 431–449. doi:10.1007/s10494-011-9378-4.

Menter, F.R., 1994. Two-equation eddy-viscosity turbulence models for engineering applications. AIAA Journal 32, 1598–1605.

Mucha, P., 2017. On Simulation-based Ship Maneuvering Prediction in Deep and Shallow Water. Ph.D. thesis. Universität Duisburg-Essen. Duisburg.

Mucha, P., el Moctar, O., Dettmann, T., Tenzer, M., 2017. Inland waterway ship test case for resistance and propulsion prediction in shallow water. Ship Technology Research 64, 106–113. doi:10.1080/09377255.2017.1349723.

Siemens, 2023. Simcenter STAR-CCM+ 2310 User Guide.